ELSEVIER

Catalysis Today 28 (1996) 49–58

CATALYSIS TODAY

Surface structures and catalytic properties of supported niobium oxides

Nobuyuki Ichikuni, Masayuki Shirai, Yasuhiro Iwasawa *

Department of Chemistry, Graduate School of Science, The University of Tokyo, Hongo, Bunkyo-ku, Tokyo 113, Japan

Abstract

Surface structures of SiO_2-supported niobium catalysts prepared by use of a Nb-monomer complex, a Nb-dimer complex, Nb pentaethoxides and Nb pentachlorides as precursors have been determined by means of EXAFS and XANES. These different Nb structures on SiO_2 have been characterized by ethanol dehydrogenation as a test reaction. In contrast to the case of Mo catalysts, the activity and selectivity of the Nb catalysts dramatically depended on the structure of the reaction sites at an atomic scale. Dynamic structural changes of the Nb sites are presented and local structural changes at the interface between the supported Nb atom and the SiO_2 surface are proposed to explain the role of support in catalysis.

Keywords: Niobium oxides; Surface structures

1. Introduction

Most catalysts used in industrial processes are robust inorganic solids, usually metal oxides or structures supported on them, which have been prepared by traditional wet-impregnation methods developed in the 1920s. As this sort of preparation cannot essentially control the structure of metal sites in general, obtained catalyst surfaces are nonuniform and difficult to characterize, and the relationship between structure and performance is often poorly defined. As a result, catalytic mechanisms are understood only at a limited macroscopic level without connection with the real reaction sites. Thus, catalytic sites have remained unidentified and, hence, efficient improvement of catalysts and catalysis has not been scientifically achieved at a molecular level.

The attached metal catalysts prepared by the reactions between suitable metal–organic and metal–inorganic complexes and inorganic oxide surfaces, followed by various controlled chemical treatments can provide useful information on the genesis of solid catalysis and a new way to develop efficient catalysts [1–6]. The use of such catalysts, which posses chemically and structurally controlled surfaces, may also shed light on catalytic mechanisms involving dynamic structural change of active sites at a molecular scale [3,6–11].

Recently, Nb oxide and its mixed oxide catalysts have been extensively studied. Niobium monomers attached on SiO_2 and TiO_2, prepared by use of $Nb(\eta^3\text{-}C_3H_5)_4$ as a precursor, have been demonstrated to be the first active catalysts for the ethanol dehydrogenation [8,12]. One

* Corresponding author.

SSDI 0920-5861(95)00228-6

monolayer niobia on SiO_2 was also prepared by the reaction of $Nb(OC_2H_5)_5$ with a SiO_2 surface [13]. EXAFS revealed the presence of a strong Nb–O–Si bonding, resulting in a structural mismatch and, hence, in coordinatively unsaturated Nb sites, which produced Lewis acidic sites [14]. More recently, the surface Nb–oxide phase was prepared by using Nb–ethoxides or Nb–oxalates as precursors and was characterized by means of in situ Raman spectroscopy [15] and FTIR [16,17]. Highly distorted NbO_6 octahedral structures were proposed for these. Datka et al. measured the concentration of Lewis acid sites and Brønsted acid sites and found they depended on the surface Nb coverage [18]. Burke and Ko prepared a series of composite oxides containing Nb_2O_5 and SiO_2 by using Nb–ethoxides and examined the relationship between acidity and structure around the Nb atom. They proposed that tetrahedral Nb species with Nb=O bonds had strong Lewis acidity and highly distorted octahedral species had only moderately strong Lewis acidity [19]. The influence of the preparation method on the structures and reactivity of the surface Nb species on SiO_2 was also investigated. Jehng and Wachs claimed that the molecular structure of the surface Nb species on SiO_2 was independent of the preparation method (oxalate, alkoxide or allyl) and gave rise to a single in situ Raman band at 980–985 cm^{-1} which was suggested to be characteristic of surface NbO_4 species with mono-oxo structure [20], different from the di-oxo structure on SiO_2 exhibiting a Raman band at 880 cm^{-1} [8,12]. These Nb catalysts produced mainly redox products (formaldehyde and methylformate) in methanol reactions [20]. They also reported that the surface Nb species on TiO_2 primarily gave rise to acidic products (dimethyl ether) [20]. Nishimura et al. demonstrated that the surface Nb species on both SiO_2 and TiO_2 prepared by use of $Nb(\eta^3\text{-}C_3H_5)_4$ yielded preferentially acetaldehyde in ethanol dehydrogenation [8].

On the SiO_2-attached Nb monomers ethanol is dehydrogenated to acetaldehyde and hydrogen, whereas on the SiO_2-attached Mo monomers and dimers ethanol is oxidatively dehydrogenated in the presence of O_2 to produce acetaldehyde and water. The difference in the reaction mode between Nb and Mo catalysts is ascribed to the difference in the Gibbs free energy for the formation of metal oxides as shown in Fig. 1 [21]. We see that MoO_3 can be reduced with H_2 but Nb_2O_5 cannot be reduced at any temperature. Again, CO can reduce MoO_3 above 800 K, but it cannot reduce Nb_2O_5 below 1600 K. Simply from Fig. 1, Nb_2O_5 resembles Ta_2O_5 rather than V_2O_5 among the group 5 elements in the periodic table.

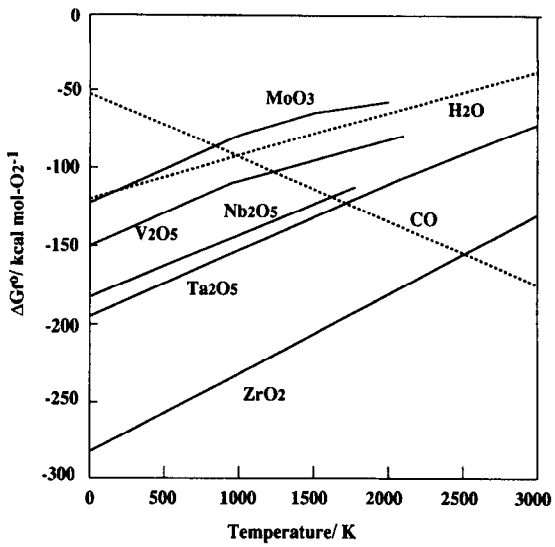

Fig. 1. Gibbs free energy of formations of Nb_2O_5, V_2O_5, Ta_2O_5, ZrO_2, MoO_3, H_2 and CO.

The authors have demonstrated that a suitable choice of Nb precursors and their supporting conditions can give rise to different designed surface Nb structures on SiO_2 which provide new insight into catalytic reaction mechanisms and essential factors for catalysis [6,8,12–14]. In this paper, improved wet methods for catalyst preparation are summarized for our Nb samples, showing that definite Nb structures composed of monomers, dimers, layers and agglomerated clusters are obtained on SiO_2. Their unique catalytic properties are also described, focusing on the catalysis by the monomers and the dimers.

2. Preparation of niobium monomer, dimer and layer catalysts

The supported Nb catalyst was prepared via the surface complex (1) which was obtained by the reaction between $Nb(\eta^3\text{-}C_3H_5)_4$ and the surface OH groups of SiO_2 (Aerosil 200; pretreated at 673 K), first at 233 K then gradually to 273 K at which temperature the system was kept for 30 min, followed by treatment with H_2 and O_2, as illustrated in Scheme 1 [8,12]. The number and character of C_3H_5 ligands and the oxidation state of Nb in the surface complex (1) were determined by chemical analysis, IR (σ-type character) and ESR (ten-line hyperfine structure derived from the 9/2 spin of Nb^{4+}). The σ-C_3H_5 ligands were removed to give rise to the lower-valent Nb species (2) which has a carbide ligand as suggested by the titration with O_2 (CO_2 formation) and also by the EXAFS analysis. The species (2) was oxidized to the Nb^{5+} state (3) with O_2 at 673 K, with uptake of a quantitative amount of oxygen. The Nb^{5+} state was also confirmed by the Nb $3d_{3/2}$ and $3d_{5/2}$ binding energies of the catalyst (3). Raman shift of (3) appeared at 880 cm^{-1} which is close to 850 cm^{-1} for tetrahedral $YNbO_4$ rather than the peak at 980 cm^{-1} for octahedral Nb_2O_5. The charge transfer band of Nb=O observed at 235 nm may also exclude the possibility of octahedral symmetry (cf, octahedral Nb_2O_5: 310 nm). The X-ray absorption near-edge structure spectrum exhibited a distinct peak assignable to the 1s → 4d transition of Nb^{5+} ions in a near tetrahedral symmetry. The bond distances and coordination numbers (CN) of the structure (3) were determined by curve-fitting analysis of the Nb K-edge EXAFS data as shown in Scheme 1. The EXAFS analysis showed the presence of the Nb–Si (surface) bond at 0.326 nm for the structure (3) besides the Nb=O bond at 0.168 nm and Nb–O bond at 0.193 nm. No Nb–Nb bonding was observed, demonstrating that the Nb^{5+} ions are distributed as isolated species (monomers). The structure is entirely different from the agglomerated Nb species (Nb–Nb: 0.314 nm; Nb–O: 0.197 nm) with an edge-shared octahedral Nb structure present in the usual Nb/SiO_2 catalyst with the identical Nb loading to 1.5 wt.-% for the Nb monomers prepared by a conventional impregnation method using a methanol solution of $NbCl_5$. As shown in Fig. 2, an aggregated structure rather than a definite dimer is obtained. Tendency for agglomeration of the Nb species was also observed on Al_2O_3, where an oligomeric corner-shared octahedral Nb structure is obtained (Fig. 2).

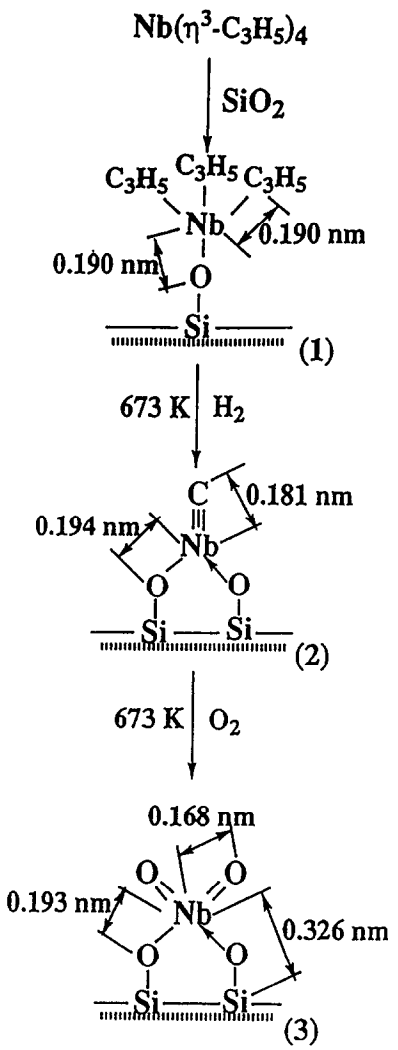

Scheme 1. Preparation steps and proposed structures of Nb monomers on SiO_2.

Niobium oxide dimers (1.0–1.5 wt.-%) were attached on two different silicas (surface areas: 200 m^2/g and 500 m^2/g) by the reaction between $[Nb(\eta^5\text{-}C_5H_5)H\text{-}\mu\text{-}(\eta^5,\eta^1\text{-}C_5H_4)]_2$ and surface OH groups of SiO_2 at 313 K, followed by decantation and washing twice by toluene to remove the unreacted complex and by evacuation to remove the residual solvent [22]. The surface Nb dimer complexes were treated with H_2 at 823 K and then exposed to a low pressure of oxygen at room temperature, followed by oxidation with O_2 at 773 K to convert them to the oxidized form [22–24]. We prepared two different Nb dimers on SiO_2 supports; one has a dimeric structure with Nb–Nb bonds at 0.303 nm bridged with oxygen on the 200 m^2/g SiO_2 and the other consists of a monomer pair without any direct Nb–Nb bonding on the 500 m^2/g SiO_2 as shown in Scheme 2 [25].

Niobium oxide monolayers on SiO_2 were prepared by using $Nb(OC_2H_5)_5$. After completion of the attaching reaction at 473 K, the sample was oxidized at 773 K. This procedure was repeated twice to cover the SiO_2 surface with Nb oxide overlayers. The Nb oxide overlayer shows two different Nb–Nb separations at

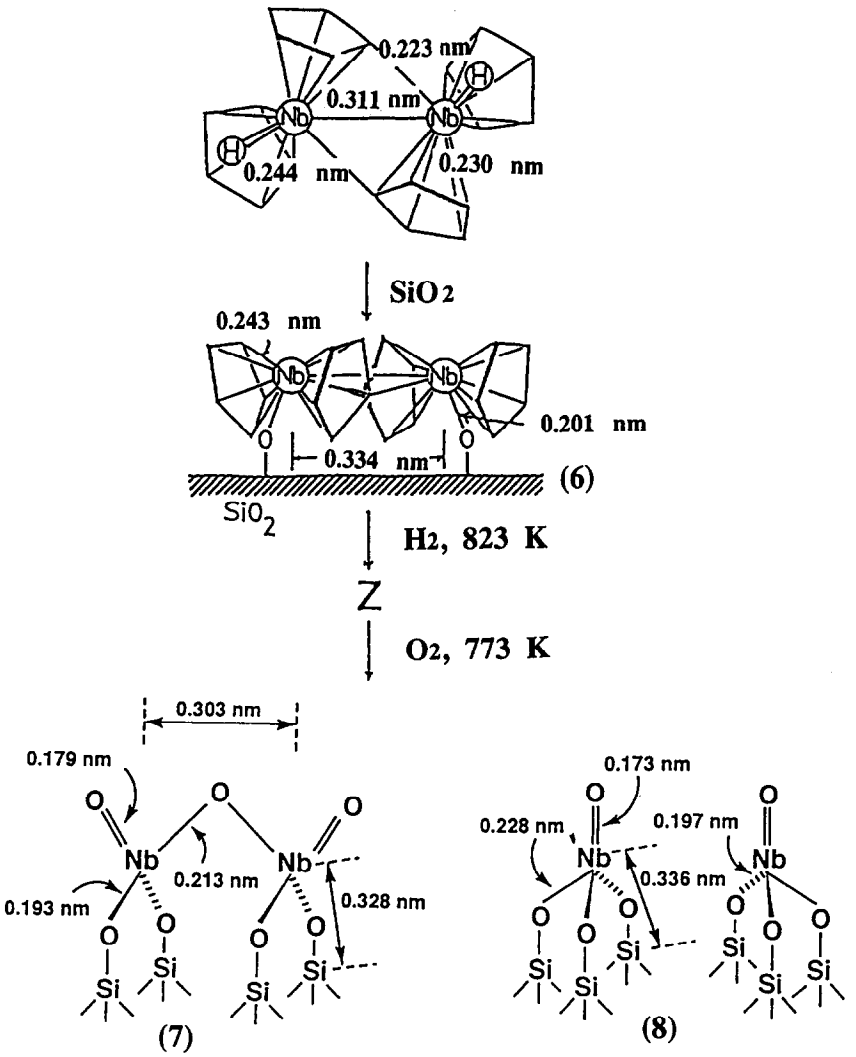

Scheme 2. Preparation steps and proposed structures of Nb dimers on SiO_2.

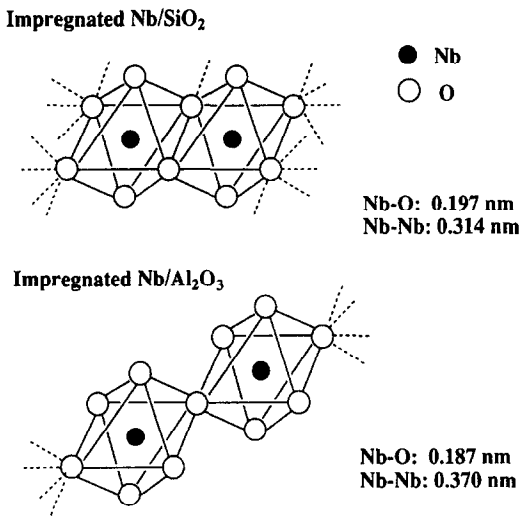

Fig. 2. Proposed units for the agglomerated Nb structures for impregnated Nb/SiO_2 and Nb/Al_2O_3 catalysts.

0.342 and 0.378 nm, both being bridged with oxygen (Nb–O = 0.211 nm) [26–28].

3. Surface catalytic dehydrogenation reaction of ethanol assisted by gas-phase ethanol

The SiO_2-supported Nb catalyst (3) exhibits a high activity and selectivity for the dehydrogenation reaction. Acetaldehyde and hydrogen were stoichiometrically produced during the reaction as shown in Fig. 3. Ethanol is dissociatively adsorbed on Nb to form $C_2H_5O(a)$ and OH(a) as proved by IR, which exhibits a peak at 3440 cm^{-1} for Nb–OH (ν(OH)) and 2979, 2935, 2900 and 2885 cm^{-1} peaks for Nb–OC_2H_5 (ν(CH)). The ν(OH) peak or ν(CH) peaks are replaced by the ν(OD) peak of 2577 cm^{-1} or the ν(CD) peaks of 2229, 2139 and 2090 cm^{-1} when ethanol is replaced by C_2H_5OD or C_2D_5OH, respectively. The peaks of adsorbed ethanol remained unchanged in vacuum, but the exchange reaction proceeded rapidly with the gas-phase ethanol. When the gas-phase ethanol was evacuated in the course of the dehydrogenation at 523 K, the reaction stopped completely as shown in Fig. 3. However, the adsorbed species still remained on the surface after evacuation of the ambient ethanol and its amount was almost the same as that adsorbed under the catalytic reaction as evidenced by the intensity of ν(OH) peak or ν(CH) peaks. Thus, the adsorbed ethanol ($C_2H_5O(a)$ + OH(a)) itself is not converted to the dehydrogenated products, $CH_3CHO + H_2$. The dehydrogenation started again by introducing ethanol vapor as shown in Fig. 3. Thus, it seemed that the reaction was assisted by the ambient ethanol. In other words, the adsorbed ethanol is stable and never reacts under vacuum at the temperatures where the catalytic reactions readily proceed.

The adsorbed ethanol was transformed only when heated to much higher temperatures than

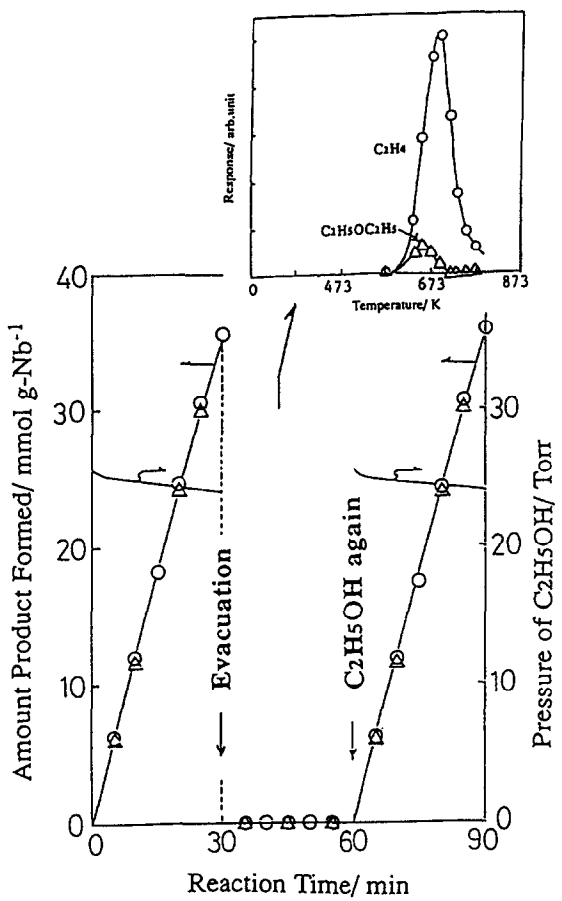

Fig. 3. Ethanol dehydrogenation on Nb/SiO_2 (3) (○: H_2, △: CH_3CHO) and TPD spectrum of adsorbed ethanol (heating rate: 4 K/min).

those operated for catalytic reactions, as shown in Fig. 3. It is to be noted in this case that the products were ethene (C_2H_4) and water (H_2O), which are entirely different from the dehydrogenated products, CH_3CHO and H_2, in the catalytic reaction of ethanol. The unimolecular-type decomposition of the adsorbed ethanol involves the breakage of γ-C–H bond of the ethoxyl group on the Nb monomer. The results demonstrate that the selectivity was switched from dehydration (γ-C–H bond breakage of the ethoxide intermediate) in vacuum to dehydrogenation (β-C–H bond breakage of the ethoxide) under gas-phase ethanol. In other words, the stable adsorbed ethanol which stoichiometrically tends to decompose to ethene and water, is activated to open a new dehydrogenation path by the presence of gas-phase ethanol, which can proceed under milder reaction conditions. How is the surface ethanol reaction assisted by gas-phase ethanol?

Ethanol was admitted onto the Nb monomers (3) to form $Nb(OH)(C_2H_5O)$ at 373 K followed by evacuation and then the system was heated at 523 K for 10 min, where no H_2 evolution was observed. When electron donating compounds were introduced to the system, the formation of H_2 and acetaldehyde started, where the pre-adsorbed ethanol was decomposed to H_2 and acetaldehyde. It is evident that the pre-adsorbed ethanol was dehydrogenated with the assistance of the post-dosed electron donors. Fig. 4 shows a linear correlation between the donor number of added nucleophilic reagents and the initial rate of H_2 (acetaldehyde) formation from the pre-adsorbed ethanol. It suggests the importance

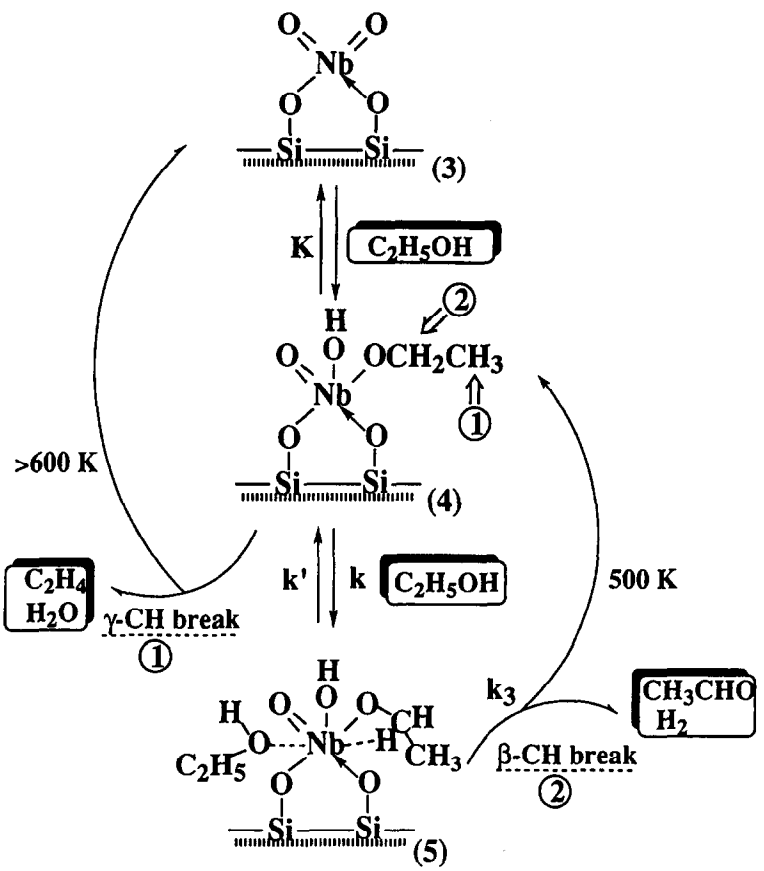

Scheme 3. Switchover of the reaction paths by gas phase ethanol.

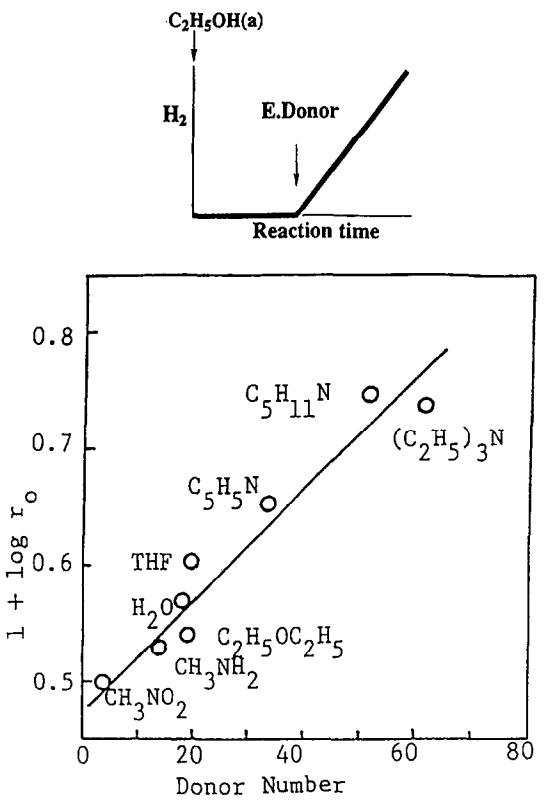

Fig. 4. Correlation between initial rates of H_2 (CH_3CHO) formation from species (4) and donor numbers of nucleophilic reagents.

of the electron donating properties of the post-dosed molecules for activating the pre-adsorbed ethanol on the Nb monomers. The rate-determining step for the ethanol dehydrogenation to form acetaldehyde is the abstraction of β-hydrogen of C_2H_5O(a) as suggested by the hydrogen isotope effect on the catalytic dehydrogenation rate of ethanol which shows that the rates for C_2H_5OH and C_2H_5OD were about 4 times higher than those for C_2D_5OH and C_2D_5OD.

The dehydrogenation mechanism is, accordingly, shown in Scheme 3. From a steady-state procedure, the following equation is derived:

$$[\mathrm{Nb}]_0/V = 1/k_3 + [(k' + k_3)/kk_3)] \times [(KP + 1)/KP^2]$$

where V, $[\mathrm{Nb}]_0$ and P represent the reaction rate, the amount of Nb monomers and the partial pressure of ethanol, respectively. Plots of $[\mathrm{Nb}]_0/V$ against $(KP + 1)/KP^2$ showed a good linear relationship [8]. This also confirms the reaction mechanism described above. The rate constant k_3 was determined to be 1.5 mmol min^{-1} g Nb^{-1}. The value approximately agrees with 1.4 mmol min^{-1} g Nb^{-1} obtained from the decomposition of species (5) under the reaction conditions at saturation of adsorption.

The present results show the switchover of the reaction path from dehydration (γ-hydrogen abstraction) to dehydrogenation (β-hydrogen abstraction) by whether or not the reaction molecules are present in gas phase, as shown in Scheme 3. The scission of β-C–H bond of a ligand in transition metal complexes has been demonstrated to be accomplished by the presence of the d electron and the preferable symmetry of C–H antibonding orbital and the d occupied orbital [29,30]. The Ti complex with a diphosphine, an ethyl and three chloro ligands is inactive for the β-C–H bond breaking because the Ti ion formally has no d electron and there is a mismatch in symmetry between the d orbital and the CH antibonding orbital. In the case of the Pd complex [29,30] the β-hydrogen can interact with the Pd atom in the same plane in the transition state and d electrons of the Pd atom can move to the CH antibonding orbital with proper symmetry overlap. The Nb^{5+} monomers (3) are incapable of abstracting the β-hydrogen in species (4) because of the d^0 ion character. Fig. 4 shows the importance of the electron donating properties of post-adsorbed molecules in species (5) for the activation of Nb^{5+} monomers in the abstraction of the β-hydrogen of C_2H_5O. Consequently, the catalytic dehydrogenation of ethanol was found to proceed with the assistance of gas phase molecules via an enhanced Nb–β-hydrogen interaction [31].

As described above, weakly adsorbed molecules under catalytic reaction conditions play an important role in surface catalytic reactions. Stable adsorbates are activated and the selectivity of the surface reaction is changed drastically under the ambient gas. The phe-

nomenon described in this article may be extended to many catalytic systems such as the water gas shift reactions, formic acid decomposition, NO–CO reaction and so on [31].

4. Catalytic behavior of the monomer pair as a dimer

It was found that the dimeric structure (7) in Scheme 2 catalyzed ethanol dehydration and contrasted with the monomeric structure which carried out dehydrogenation (3). The switchover in the selectivity of the Nb site occurred because of replacement of the second ethanol molecule in species (5) of Scheme 3 by a second Nb atom. It is to be noted that control of catalysis is, thus, possible by atomic-scale regulation of the number of Nb atoms involved in the reaction sites. We also found that Nb monomer-pairs (8) with each Nb site being a monomer catalyzed the dehydration rather than the dehydrogenation. The structure (8) in Scheme 2 is similar to that for the Nb monomer on TiO_2 [8]. The selective dehydration of ethanol on the catalyst (8) is strange because the monomers on SiO_2 and TiO_2 behave as dehydrogenation catalysts. The reason for the change

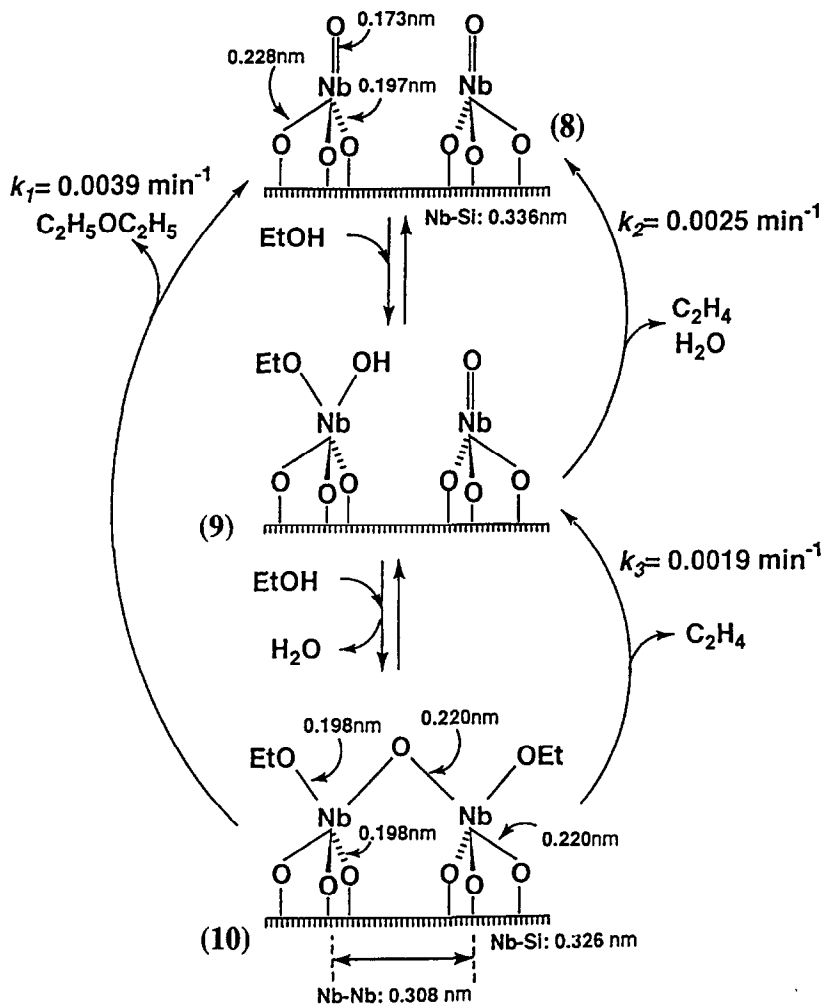

Scheme 4. Reaction mechanism for ethanol dehydration on the catalyst (8).

in selectivity was a dynamic structure change in the Nb sites in the course of the dehydration reaction as summarized below [24,25].

The structural change of the Nb sites during catalytic ethanol dehydration was examined by EXAFS. The quantitative formation of H_2O equivalent to the number of Nb monomer-pairs was observed in the initial stage of reaction. After the rapid formation of water, the steady state dehydration reaction proceeded. Upon the rapid formation of water, the Nb=O double bond disappeared and a new Nb–Nb bond of 0.308 nm with the coordination number of one appeared. Ethanol adsorbed on the Nb=O sites, producing Nb–OH and Nb–OC_2H_5 [23]. When Nb–OH species, thus, formed were located close to each other, dehydration readily took place at 523 K. As a result, Nb–O–Nb bonds were formed to make a dimeric structure as shown in Scheme 4. The coordination number of Nb–O of 0.198 nm was determined to be 3.2 which is larger by 0.6 than 2.6 for the original catalyst (8). It suggests that an additional Nb–O bond at 0.198 nm (Nb–OC_2H_5) was formed upon ethanol adsorption, which agrees with the results of IR and XANES. The IR spectra at this stage showed the ν(CH) peaks of Nb–OC_2H_5, but no ν(OH) peak of Nb–OH [25]. Accordingly, the structural change by ethanol adsorption at 523 K accompanied with water evolution is illustrated in Scheme 4 [25].

When the Nb dimers (10) fully adsorbed with ethanol were decomposed, ethene and diethyl ether were evolved, regenerating the Nb=O bonds and breaking the Nb–Nb bonds as proved by EXAFS. It is suggested in Scheme 4 that the dehydration of ethanol on the catalyst (8) proceeds in conjunction with a dynamic structural change in the Nb sites involving formation and breaking of Nb–O–Nb bonds.

It is to be noted that the Nb–Si separation changed from 0.336 nm for the monomeric structure (8) to 0.326 nm for the dimeric structure (10) by ethanol adsorption, while the longest Nb–O (surface) bond was shortened from 0.228 nm for the catalyst (8) to 0.220 nm for (10) upon ethanol adsorption in Scheme 4 [25]. These results suggest that the bond angles of Nb–O–Si and O–Nb–O became narrower and wider, respectively, by a local rearrangement involving the movement of a Nb atom to the longest O atom and the rearrangement of the Si sites at the topmost SiO_2 surface. We propose that an appropriate flexibility of the interface structure may assist the dynamic change of active Nb structures during the catalysis, which may be a role for the support surface in selective catalysis. Reversible local-structure changes at the interface important for efficient catalysis will be reported elsewhere [32].

References

[1] Yu.I. Yermakov, B.N. Kuznetsov and V.A. Zakharov, Catalysis by Supported Complexes, Elsevier, Amsterdam, 1981.
[2] Y. Iwasawa (Editor), Tailored Metal Catalysts, Reidel, Dordrecht, 1986.
[3] Y. Iwasawa, Adv. Catal., 35 (1987) 187.
[4] B.C. Gates, L. Guczi and H. Knozinger (Editors), Stud. Surf. Sci. Catal., 29 (1986).
[5] F.R. Hertly, Supported Metal Complexes, Reidel, Dordrecht, 1985.
[6] Y. Iwasawa, Catal. Today, 18 (1993) 21.
[7] Y. Iwasawa, K. Asakura, H. Ishii and H. Kuroda, Z. Phys. Chem., 144 (1985) 105.
[8] M. Nishimura, K. Asakura and Y. Iwasawa, Proc. 9th Int. Congr. Catal., IV (1988) 1842.
[9] Y. Izumi, T. Chihara, H. Yamazaki and Y. Iwasawa, J. Phys. Chem., 98 (1994) 594.
[10] Y. Izumi and Y. Iwasawa, CHEMTECH, 24 (1994) 20.
[11] N. Ichikuni and Y. Iwasawa, J. Phys. Chem., 98 (1994) 11576.
[12] M. Nishimura, K. Asakura and Y. Iwasawa, J. Chem. Soc., Chem. Commun., (1986) 1660.
[13] K. Asakura and Y. Iwasawa, Chem. Lett., (1986) 859.
[14] K. Asalura and Y. Iwasawa, J. Phys. Chem., 95 (1991) 1711.
[15] J.M. Jehng and I.E. Wachs, J. Phys. Chem., 95 (1991) 7373.
[16] A.M. Turek, I.E. Wachs and E. DeCanio, J. Phys. Chem., 96 (1992) 5000.
[17] M.A. Vuurman and I.E. Wachs, J. Phys. Chem., 96 (1992) 5008.
[18] J. Datka, A.M. Turek, J.M. Jehng and I.E. Wachs, 135 (1992) 186.
[19] P.A. Burke and E.I. Ko, J. Catal., 129 (1991) 38.
[20] J.M. Jehng and I.E. Wachs, Catal. Today, 16 (1993) 417.
[21] T.B. Reed, Free Energy of Formation of Binary Compounds, MIT Press, Cambridge, 1971.
[22] N. Ichikuni, K. Asakura and Y. Iwasawa, J. Chem. Soc., Chem. Commun., (1991) 112.

[23] N. Ichikuni and Y. Iwasawa, Proc. 10th Int. Congr. Catal., A (1993) 477.
[24] N. Ichikuni and Y. Iwasawa, Catal. Today, 16 (1993) 427.
[25] N. Ichikuni and Y. Iwasawa, J. Phys. Chem., 98 (1994) 11576.
[26] K. Asakura and Y. Iwasawa, Chem. Lett., (1986) 859.
[27] K. Asakura and Y. Iwasawsa, Chem. Lett., (1988) 633.
[28] K. Asakura and Y. Iwasawa, J. Phys. Chem., 95 (1991) 1711.
[29] Z. Dawoodi, M.L.H. Green, V.S.B. Mtetwa and K. Prout, J. Chem. Soc., Chem. Commun., (1982) 802.
[30] N. Koga, S. Obara, K. Kitaura and K. Morokuma, J. Am. Chem. Soc., 107 (1985) 7109.
[31] Y. Iwasawa, Acc. Chem. Res., in press.
[32] K. Okumura, K. Asakura and Y. Iwasawa, to be published.